ELSEVIER

Catalysis Today 73 (2002) 233–238

CATALYSIS TODAY

www.elsevier.com/locate/cattod

Towards the comprehension of oxygen storage processes on model three-way catalysts

Sumeya Bedrane*, Claude Descorme, Daniel Duprez

Laboratoire de Catalyse en Chimie Organique (LACCO), UMR CNRS 6503, Université de Poitiers, 40 Avenue du Recteur Pineau, 86022 Poitiers Cedex, France

Abstract

CeO_2- and $Ce_{0.63}Zr_{0.37}O_2$-supported noble metal catalysts were studied. Samples were fully characterized using TEM, XRD, N_2 adsorption and H_2 chemisorption. The oxygen storage process was investigated focusing on the evolution as a function of temperature of both the oxygen storage capacity (OSC) and the oxygen storage complete capacity (OSCC). Aging effect on OSC was also examined in details in the case of Rh catalysts. Finally, the major role of oxygen diffusion, partly influenced by the metal/support interface quality, was confirmed. © 2002 Elsevier Science B.V. All rights reserved.

Keywords: Three-way catalysts; Oxygen storage capacity; Oxygen storage complete capacity

1. Introduction

Nowadays, increasing attention is being paid to the environment. As a matter of fact, the automobile sector is a major contributor to the atmospheric pollution and many studies have been devoted to the optimization of catalytic converters [1]. Since the 1990s, numerous studies have been devoted to the study of ceria–zirconia mixed oxides, used as oxygen storage components in three-way catalysts (TWC). Investigations dealt with preparation methods [2,3], thermal stability [4], structural properties [5,6] and redox behavior [7,8]. Many papers were also dedicated to oxygen storage capacity measurements [9–11]. However, only a few works concentrated on the comprehension of the oxygen storage process itself [12].

2. Experimental

Cerium oxides (CeO_2 and $Ce_{0.63}Zr_{0.37}O_2$) were supplied by Rhodia Electronics and Catalysis (La Rochelle, France). Oxides were pre-calcined at 900 °C for 6 h. Metal precursors ($Rh(NO_3)_3$, $Pt(NH_3)_4(OH)_2$, $Pd(NO_3)_3$, $Ru(NO)(NO_3)_3$ and $Ir[CH(COCH_3)_2]_3$) were impregnated on the supports at room temperature. Metal loading was fixed at about 100 μmol of metal atoms per gram of catalyst: 1 wt.% for Rh, Pd and Ru and 2 wt.% for Pt and Ir. Samples were dried at 120 °C for 24 h and finally pretreated for 4 h at 500 °C under flowing air or hydrogen (30 $cm^3\,min^{-1}$). Catalysts were further aged under different conditions (Table 1).

Catalysts composition was checked by Elemental Analysis (Service Central d'Analyses du CNRS, France) and energy dispersive X-rays (EDX). The sample structure was investigated using a Siemens D5005 diffractometer. Crystalline phases were identified by comparison with ICDD files. The average crystallite size was calculated from the Scherrer equation. Surface areas were measured by N_2 adsorption at −196 °C (single point method) with a Micromeritics Flowsorb II apparatus. Transmission electron microscopy direct observations of the pre-reduced samples were carried out on a CM 120 Philips

* Corresponding author.

0920-5861/02/$ – see front matter
PII: S0920-5861(02)00005-6

Table 1
Metal dispersion of fresh and aged catalysts

	CeO_2			$Ce_{0.63}Zr_{0.37}O_2$		
	Fresh, *D* (%)	Aged		Fresh, *D* (%)	Aged	
		D (%)	Aging		*D* (%)	Aging
Rh	88[a]	5[a]	800 °C (H_2)	62[a]	8[a]	1000 °C (H_2)
Pt	79[a]	37[a]	800 °C (air)	78[a]	6[a]	1000 °C (air)
Pd	78[a]	10[b]	900 °C (H_2)	61[a]	55[b]	800 °C (air)
Ru	60[b]	38[b]	800 °C (H_2)	82[b]	44[b]	800 °C (H_2)
Ir	38[a,b]	3[a]	700 °C (air)	29[a,b]	2[a]	700 °C (air)

[a] Estimated from H_2 chemisorption measurements.
[b] Estimated from TEM direct observations.

microscope. An average size of the metal particles was estimated from TEM micrographs. Metal dispersions were also calculated from H_2 chemisorption measurements carried out in a home-made apparatus described elsewhere [13]. After 1 h reduction and 3 h outgassing at 400 °C, H_2 chemisorption was measured at −85 °C following an optimized procedure [14].

Oxygen storage capacities were measured based on a method earlier presented by Yao and Yu Yao [15] and further adapted by Duprez and coworkers [13]. Experiments were carried out in a pulse chromatographic system [12]. The oxygen storage capacity (OSC) corresponds to the most "reactive" and the most available oxygen atoms. The oxygen storage complete capacity (OSCC) represents the maximum reducibility of sample. Both values are expressed in μmoles of CO_2 produced by gram of sample.

3. Results and discussion

3.1. Textural and structural characteristics

The main characteristics for bare oxides and fresh catalysts were reported earlier [12]. XRD characterizations confirmed that both CeO_2 and $Ce_{0.63}Zr_{0.37}O_2$ are purely monophasic samples with a fluorite-type structure ($a = 5.4113$ and 5.3044 Å, respectively). $Ce_{0.63}Zr_{0.37}O_2$ exhibits the highest thermal stability [16]. Looking at supported catalysts, the metallic phase dispersion was estimated for both "fresh" and "aged" catalysts using H_2 chemisorption measurements and/or TEM direct observations. In the case of ruthenium and palladium catalysts, dynamic hydrogen chemisorption was not suitable. For iridium catalysts, both methods were used to evaluate metal particle size. As earlier showed, the hydrogen chemisorption stoichiometry on Ir was assumed to be 3 [17]. For the other noble metals, metal dispersions were calculated assuming a stoichiometry H/Ms equals to 1. The main results are summarized in Table 1.

On the fresh catalysts, the metallic phase is well dispersed. The average particle size varies between 10 and 30 Å. Upon aging, sintering occurs and the dispersion decreases drastically. In fact, aging conditions were adjusted, depending on the metal and the support, in order to obtain strongly sintered catalysts. Nevertheless, one can see that some catalysts could hardly be sintered. This enhanced stability of some of the metals would be related to an effective metal–support interaction.

3.2. Oxygen storage complete capacity

Measurements consist in a sequence of CO pulses up to the maximum reduction of the sample. The evolution of the CO uptake as a function of the number of pulses is shown in Fig. 1 for two different Ru catalysts.

Whatever the support, maximum reduction is not instantaneous. In the case of Ru/CeO_2, four CO pulses are necessary before getting to the saturation point. For $Ru/Ce_{0.63}Zr_{0.37}O_2$, CO consumption never goes to zero. This continuous consumption could be explained by the participation of bulk oxygen atoms to the OSC process.

OSCC measurements demonstrated the difference in the reducibility of ceria and ceria–zirconia mixed oxides. Considering the OSCC values at 500 °C, the

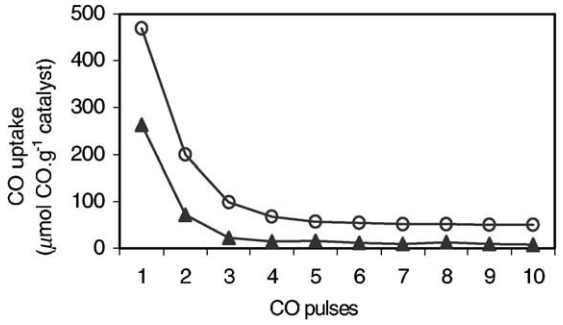

Fig. 1. Evolution of the CO uptake at 200 °C as a function of the number of CO pulses on Ru/CeO_2 (▲) and $Ru/Ce_{0.63}Zr_{0.37}O_2$ (○) fresh catalysts.

reduced oxides chemical formula would be $CeO_{1.97}$ and $Ce_{0.63}Zr_{0.37}O_{1.85}$. Additionally, by comparison with the results obtained on bare oxides, Ru metal particles were shown to be responsible for an enhanced reducibility of the support.

3.3. Oxygen storage capacity

Influence of temperature on OSC earlier showed that: (i) in the case of ceria-based catalysts, OSC varies slightly with temperature and reaches a maximum corresponding to the full reduction of the oxide surface and (ii) in the case of $Ce_{0.63}Zr_{0.37}O_2$-supported catalysts, oxygen storage is strongly activated by temperature and bulk reduction is responsible for the observed OSC enhancement. In both cases, storage was concluded to be governed by diffusion, either at the surface or in the bulk of the oxide [12].

In this study, the influence of metal particles size and the role of the metal/oxide interface were checked. OSC at 400 °C of fresh and aged catalysts are compared in Table 2.

The results reported in Table 2 show a decrease of the OSC upon aging, except for $Rh/Ce_{0.63}Zr_{0.37}O_2$ and $Ru/Ce_{0.63}Zr_{0.37}O_2$. In fact, metal particles act as portholes for the subsequent migration and storage of oxygen onto the support. As a result, OSC would depend on the metallic area, that is the dispersion (Table 1). Nevertheless, no direct correlation could be found.

Looking at Fig. 2, we observed that the evolution of the OSC as a function of temperature for both fresh and aged catalysts follows the same trend. OSC is decreased by almost the same amount in the whole range of temperature. Upon aging, the number and/or the accessibility of the active sites involved in the storage process is/are decreased.

Table 2
Influence of aging on the oxygen storage capacity

	OSC at 400 °C (μmol CO_2 g^{-1})			
	CeO_2		$Ce_{0.63}Zr_{0.37}O_2$	
	Fresh	Aged	Fresh	Aged
Rh	257	142	858	1147
Pt	153	116	823	531
Pd	167	80	832	749
Ru	254	243	940	967
Ir	363	99	994	541

Previously, calculating the number of oxygen layers (NL) involved in the storage process at 500 °C, we demonstrated that oxygen storage is restricted at the surface of ceria-supported catalysts, whereas in the case of $Ce_{0.63}Zr_{0.37}O_2$ mixed oxide-based catalysts several bulk oxygen layers do participate [12]. In this study, we calculated the number of oxygen layers involved in the storage process to be 5.2 and 4.2 for the fresh and aged $Pt/Ce_{0.63}Zr_{0.37}O_2$ catalysts, respectively. Even after severe aging, bulk reduction still proceeds. For Pt/CeO_2 catalysts, oxygen storage is still strictly limited at the surface of ceria (NL: 0.6 for the fresh catalyst and 0.5 for the aged one).

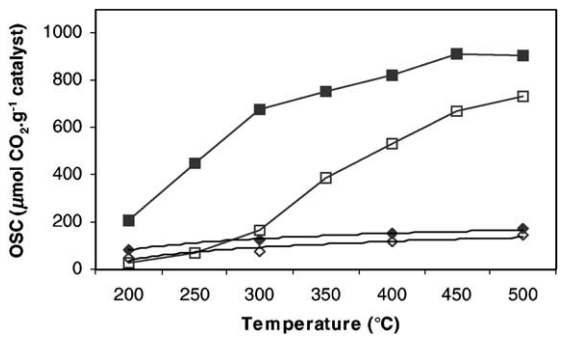

Fig. 2. Evolution of OSC as a function of temperature on Pt/CeO_2 (◆) and $Pt/Ce_{0.63}Zr_{0.37}O_2$ (■) catalysts—influence of metal particle size (fresh catalysts: closed symbols, aged catalysts: open symbols).

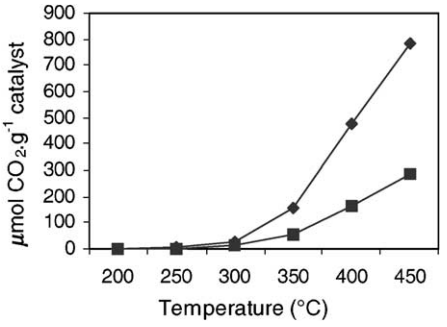

Fig. 3. Evolution of OSC (■) and OSCC (◆) as a function of temperature on bare $Ce_{0.63}Zr_{0.37}O_2$ oxide.

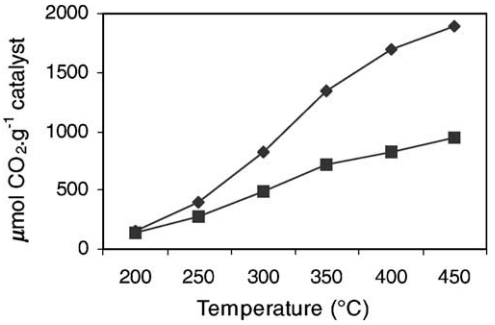

Fig. 4. Evolution of OSC (■) and OSCC (◆) as a function of temperature on a $Pd/Ce_{0.63}Zr_{0.37}O_2$ catalyst.

3.4. OSCC vs. OSC

To better understand the storage process and the role of the different functions of the catalyst, evolutions of both the OSC and the OSCC as a function of temperature were compared (Figs. 3 and 4).

Results displayed in Fig. 3 show that oxygen storage does not proceed before 300 °C on bare oxides. Above this temperature, oxygen storage sites on the surface may be accessed. As temperature increases, the discrepancy between OSC and OSCC increases. OSC is limited by the number of the most reactive species probably located at the oxide surface, while OSCC represents the maximum reducibility of the oxide. Considering the OSCC values, it clearly appears then that, in the case of mixed oxides, bulk oxygen atoms may participate in the oxygen storage process.

On the opposite, in the presence of metal particles (Fig. 4), oxygen storage may proceed even at relatively low temperature. Around 200 °C, oxygen storage is limited to the metal particle and its very close vicinity. OSC and OSCC values are identical. Above that temperature, the same trend as for bare oxides is observed. By comparison between these two figures, it clearly appears that the reducibility of the oxides is widely enhanced in the presence of metal particles. Furthermore, one can see that OSC is enhanced in the whole range of temperature. At 500 °C, the number of the most reactive species would have been multiplied by a factor of at least 3. Another explanation would be that the metal particles act as "portholes" or "activators" for the subsequent migration and storage of oxygen onto the support. The important role of the metal–support interaction that is the metal–support interface and the interfacial perimeter is clearly exemplified.

3.5. Aging effect

To go further in the analysis of aging effects on the OSC, a $Rh/Ce_{0.63}Zr_{0.37}O_2$ catalyst was submitted to several aging pretreatments. The main details and characteristics of the catalysts are presented in Table 3.

To check the influence of an increase of metal particle size, OSC of the four samples were measured in the same conditions. Results are reported in Fig. 5.

Table 3
Dispersion of Rh phase on aged $Rh/Ce_{0.63}Zr_{0.37}O_2$ samples

Sample	Aging conditions			Dispersion (%)[a]	Particle size (Å)[a]
	Gas	Temperature (°C)	Time (h)		
Rh/CeZr-1 (fresh)	Air	500	4	62	15
Rh/CeZr-2 (aged)	Air	800	4	55	16
Rh/CeZr-3 (aged)	Air	900	4	14	65
Rh/CeZr-4 (aged)	H_2	1000	4	8	113

[a] Calculated from H_2 chemisorption measurements.

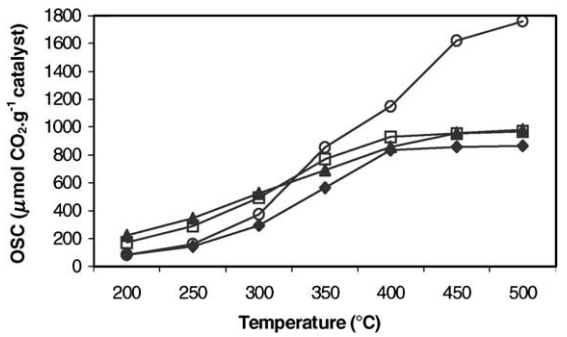

Fig. 5. Aging effects on the OSC evolution as a function of temperature for a series of $Rh/Ce_{0.63}Zr_{0.37}O_2$ catalysts ((▲) Rh/CeZr-1, (□) Rh/CeZr-2, (◆) Rh/CeZr-3, (○) Rh/CeZr-4)).

In the interval between 200 and 300 °C, OSC is restricted to the metal oxido-reduction and depends on the dispersion. Above 300 °C, OSC is essentially due to the support participation. At low temperature, a constant decrease of the OSC is observed as the metal dispersion decreases, except for the fourth sample. For Rh/CeZr-4, OSC was unexpectedly enhanced. In fact, OSC at 500 °C is about twice the OSC of the fresh Rh/CeZr-1 catalyst (1760 vs. 980 μmol CO_2 g^{-1} catalyst). In fact, Vidal et al. [18] earlier evidenced the beneficial effect of severe reduction on the overall reducibility of $Ce_{0.68}Zr_{0.32}O_2$. This phenomenon was explained by a modification of the oxygen sub-lattice induced either by a high structural disorder in the cubic oxygen sub-lattice or a different geometry of the Ce–O/Zr–O bonds. In our case, that is in the presence of metal particles, such an increase of the OSC could also be attributed to structural modifications of the metallic phase upon aging. Gatica et al. [19] earlier reported that metal decoration by the support and/or electronic metal–support interaction could occur upon $Rh/Ce_{0.68}Zr_{0.32}O_2$ reduction at temperature higher than 500 °C.

A closer look to the results shows that the Rh/CeZr-4 behavior diverges from the "expected" behavior when the oxide starts participating in the oxygen storage process ca. 300 °C (see Fig. 3). This observation indicates that the metal/support interface and/or the support have been modified in such a way that oxygen transfer to and from the support and/or oxygen diffusion and storage would be favored.

To further analyze this result, Rh/CeZr-4 was fully characterized using surface area measurements, X-rays diffraction and H_2 chemisorption.

Diffractograms displayed in Fig. 6 clearly show a decrease of the FWHM of the diffraction peaks upon aging. The main characteristics of these two samples are summarized in Table 4.

In the absence of demixtion, these modifications evidence a crystallization of the oxide upon aging. As a result, oxygen diffusion could occur on a larger length scale and, consequently, oxygen storage would be enhanced. On the opposite, Boaro et al. [20] reported that bare oxide sintering causes the deterioration of the OSC of ceria and ceria–zirconia mixed oxides. Thus, the presence of rhodium particles would prevent deactivation upon aging [21]. "New" metal–support interactions at the interface would be responsible for the OSC enhancement.

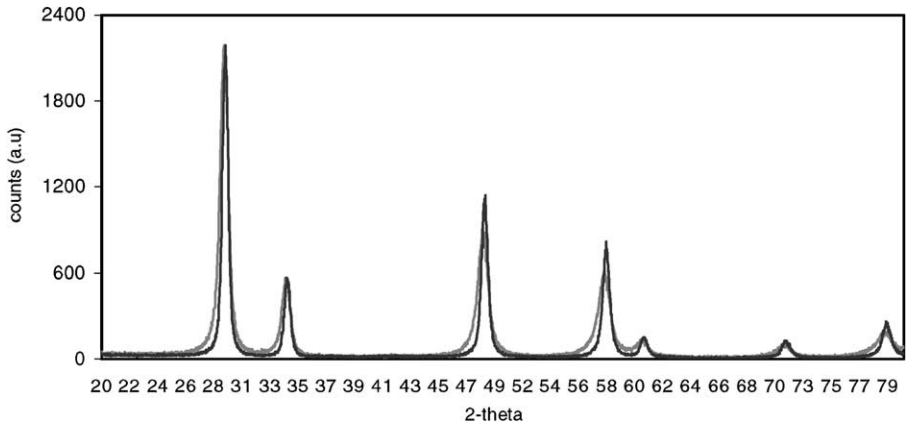

Fig. 6. Aging effect on the oxide support structure: Rh/CeZr-1 (gray) and Rh/CeZr-4 (black).

Table 4
Influence of aging on $Rh/Ce_{0.63}Zr_{0.37}O_2$ structural and textural characteristics

Catalyst	S_{BET} ($m^2\ g^{-1}$)	Oxide particle size (Å)[a]	Metal particle size (Å)[b]
Rh/CeZr-1 (fresh)	38	80	15
Rh/CeZr-4 (aged)	23	134	113

[a] Estimated from XRD analysis.
[b] Calculated from H_2 chemisorption measurements.

4. Conclusions

Ceria–zirconia mixed oxide was shown to be highly reducible. In the presence of metal particles, oxides reducibility is enhanced. Furthermore, depending on aging conditions, two different behaviors were identified: (i) for most catalysts, oxygen storage sites are "destroyed" (decreased accessibility, structural modifications, metal particles sintering, etc.) and OSC decreases upon aging, (ii) for $Rh/Ce_{0.63}Zr_{0.37}O_2$ catalyst, OSC at temperature higher than 300 °C is enhanced after severe reduction. Beneficial modifications of the metal–support interface and/or the oxide structure are responsible for such an unexpected behavior. Oxygen activation and transfer is facilitated (metallic phase) and diffusion occurs on a larger length scale (oxide).

References

[1] J. Barbier Jr., D. Duprez, Appl. Catal. B 4 (1994) 105.
[2] D. Terribile, A. Trovarelli, J. Llorca, C. De Leitenburg, G. Dolcetti, Catal. Today 43 (1998) 79.
[3] S. Rossignol, F. Gerard, D. Duprez, J. Mater. Chem. 9 (1999) 1615.
[4] G. Colon, F. Valdiviesco, M. Pijolat, R.T. Baker, J.J. Calvino, S. Bernal, Catal. Today 50 (1999) 271.
[5] G. Vlaic, P. Fornasiero, S. Geremia, J. Kaspar, M. Graziani, J. Catal. 186 (1997) 386.
[6] M. Fernandez-Garcia, A. Matines-Arias, A. Iglesias-Juez, C. Belver, A.B. Hungria, J.C. Conesa, J. Soria, J. Catal. 194 (2000) 385.
[7] P. Fornasiero, G. Balducci, R. Di Monte, J. Kaspar, V. Sergo, G. Gubitosa, A. Ferrero, M. Graziani, J. Catal. 164 (1996) 173.
[8] M. Daturi, E. Finocchio, C. Binet, J.C. Lavalley, F. Fally, V. Perrichon, J. Phys. Chem. B 103/123 (1999) 4884.
[9] T. Murota, T. Hasegawa, S. Aozasa, H. Matsui, M. Motoyama, J. Alloys Comp. 193 (1993) 298.
[10] J.P. Cuif, G. Blanchard, O. Touret, A. Seigneurin, M. Marczi, E. Quemere, Society of Automotive Engineers Technical Paper Series, Paper No. 970463, 1997.
[11] A. Trovarelli, F. Zamar, J. Llorca, C. De Leitenburg, G. Dolcetti, J.T. Kiss, J. Catal. 169 (1997) 490.
[12] S. Bedrane, C. Descorme, D. Duprez, Catal. Today, in press.
[13] S. Kacimi, J. Barbier Jr., R. Taha, D. Duprez, Catal. Lett. 22 (1993) 343.
[14] Y. Madier, Ph.D. Thesis, Poitiers University, 1999.
[15] H.C. Yao, Y.F. Yu Yao, J. Catal. 86 (1984) 254.
[16] Y. Madier, C. Descorme, A.M. Le Govic, D. Duprez, J. Phys. Chem. B 103/150 (1999) 10999.
[17] S. Bedrane, C. Descorme, D. Duprez, J. Mater. Chem., submitted for publication.
[18] H. Vidal, S. Bernal, J. Kaspar, M. Pijolat, V. Perrichon, G. Blanco, J.M. Pintado, R.T. Baker, G. Colon, F. Fally, Catal. Today 54 (1999) 93.
[19] J.M. Gatica, R.T. Baker, P. Fornasiero, S. Bernal, G. Blanco, J. Kaspar, J. Phys. Chem. B 104 (2000) 4667.
[20] M. Boaro, C. De Leitenburg, G. Docetti, A. Trovarelli, J. Catal. 193 (2000) 338.
[21] S. Bedrane, C. Descorme, D. Duprez, Stud. Surf. Sci. Catal. 138 (2001) 125.